PHYSICAL REVIEW E **75**, 056303 (2007)

Magnetic Field Driven Instability in Stratified Ferrofluids

Andrey Ryskin and Harald Pleiner
Max-Planck-Institut für Polymerforschung, D 55021 Mainz, Germany

We describe a convective instability of a stratified ferrofluid subject to a magnetic field. The ferrofluid is described as binary mixture featuring two important dimensionless numbers, B the barometric and B_m the magnetic barometric one. At the field strength, where the latter exceeds the former, instability sets in. We discuss the growth rate of linear perturbations and the amplitude of nonlinear stationary convection rolls. The latter is governed by the balance of concentration advection and sedimentation.

PACS numbers: 47.20.-k, 44.27.+g, 75.50.Mm DOI: 10.1103/PhysRevE.75.056303

I. INTRODUCTION

Ferrofluids, the stable suspension of nano-sized magnetic particles in a carrier fluid, are generally treated as a one-component fluid [1–6]. This is because the concentration dynamics of the magnetic nanoparticles is extremely slow. However, it cannot be neglected when one deals with thermal instabilities [7–10]. Instead, one has to consider the ferrofluid as a binary mixture. Thermal instabilities in binary mixtures have been investigated for a long time [11–13]. In comparison to the pure fluid case, the dynamics and the bifurcation scenario are more complicated due to the extra degree of freedom associated with the concentration field. Compared to usual molecular binary mixtures, however, ferrofluids are atypical, because the two constituents have very different densities and show very different mobilities due to the large size of the magnetic particles on the molecular lengthscale. In earth's (vertical) gravity field, the density difference is responsible for rather strong sedimentation effects in ferrofluids which are generally negligible in molecular binary mixtures. For thermal instabilities, with a temperature gradient along gravity, sedimentation is a stabilizing effect on the system, since the heavier constituent accumulates at the bottom, thus counteracting thermal buoyancy. Recent experiments show that sedimentation strongly effects the qualitative behavior of thermal instabilities [14–16]. In this communication we will show, however, that even without a temperature gradient a stratified ferrofluid can become unstable, if a strong enough external magnetic field is applied along the concentration gradient. This novel type of sedimentation instability is due to the Kelvin force, which is larger in areas with higher concentration of magnetic particles. Concentration fluctuations are therefore amplified and can lead to an instability.

II. SETTING OF THE PROBLEM

Let us consider a horizontal layer of ferrofluid between two rigid impermeable plates and subject to a gravitational field $\boldsymbol{g} = g\,\boldsymbol{e}_g$ along the negative z direction. If one waits long enough, the concentration distribution of the magnetic particles becomes exponential in vertical direction [17] $C(z) = C_0 \exp(-z/h_s)$. In the dilute limit this is essentially a Boltzmann distribution with the sedimentation length $h_s = k_B T/(m_p g)$, where m_p is the mass of the magnetic particles. If h_s is much larger than the distance between the two plates, h, which is usually the case in experiments, we can expand this exponential distribution and get a linear concentration profile $C(z) = \overline{C}_0(1 - z/h_s)$, where $\overline{C}_0$ is the mean volume fraction of the magnetic particles between the plates at $z = \pm h/2$.

After the concentration distribution is equilibrated, a magnetic field in vertical direction is switched on. Then we study the linear and nonlinear evolution of the perturbations of the steady and flow-free system.

The general system of dynamic equations to describe ferrofluids with concentration variations in magnetic field has been derived in [9]. In order to include sedimentation effects one needs to add the appropriate mass flux to the concentration dynamics [18]

$$\boldsymbol{j}_s = \frac{D_c}{h_s} C\,\boldsymbol{e}_g, \tag{1}$$

where D_c is the concentration diffusion coefficient. As it is often done we neglect the dependence of the flux on concentration variations and take $C = \overline{C}_0$ in Eq. (1). In this case the flux due to sedimentation is constant, its gradients vanish, and it only shows up in the impermeability condition at the horizontal plates.

Since there is no external temperature gradient applied, we can assume the system to be isothermal and drop the thermal degree of freedom from the list of macroscopic variables. This also eliminates any cross-coupling between temperature variations and the remaining variables, which are the concentration C, the velocity $\boldsymbol{v}$, and the magnetic field. For the latter we introduce scalar potentials ϕ and ϕ_e, for the magnetic field inside and outside the ferrofluid layer, respectively.

Since we cannot use thermal quantities to make the macroscopic equations dimensionless, we use the following scaling factors: h for any length, h^2/ν for the time (with ν the kinematic viscosity of the ferrofluid), $\overline{C}_0 h/h_s$ for the concentration and $H_0\chi_c\overline{C}_0 h^2/(h_s\bar{\epsilon})$ for the magnetic potentials. Here,

$\chi_c = \partial\chi/\partial C$ describes the concentration dependence of the magnetic susceptibility χ of the ferrofluid giving rise to magnetophoresis, H_0 is the strength of the applied magnetic field within the ferrofluid ($H_0(1+\chi)$ is the externally applied field), and $\bar{\epsilon}$ is the effective magnetic permeability (see below). This procedure reduces the macroscopic dynamic bulk equations of Ref. [9] to

$$\left[\frac{\partial}{\partial t} + (\boldsymbol{v}\cdot\nabla)\right] C - \frac{1}{Sc}\Delta(C - M_f\nabla_z\phi) = 0 \qquad (2)$$

$$\left[\frac{\partial}{\partial t} + (\boldsymbol{v}\cdot\nabla) - \Delta\right] (\mathrm{curl}\,\boldsymbol{v})_i + B\,\epsilon_{ikz}\nabla_k C + B_m\,\epsilon_{ikl}(\nabla_l\nabla_z\phi)\nabla_k C = 0 \qquad (3)$$

$$\left[\nabla_z^2 + M_3(\nabla_x^2 + \nabla_y^2)\right]\phi - \nabla_z C = 0 \qquad (4)$$

describing concentration diffusion and magnetophoresis in Eq. (2), where the former is governed by the Schmidt number $Sc = \nu/D_c$ and the latter by $M_f = \chi_c^2 H_0^2/(\gamma_H\bar{\epsilon})$ with γ_H, the stiffness coefficient of concentration variations, defined by $\gamma_H = \partial^2 f/(\partial C)^2$ with f the energy density [19]. Generally, in ferrofluids M_f is smaller than unity [20].

In the flow equation (3), amended by incompressibility $\mathrm{div}\,\boldsymbol{v} = 0$, there are two important parameters for the problem

$$B = \frac{\alpha_c g\,\overline{C}_0 h^4}{\nu^2 h_s} \quad \text{and} \quad B_m = \frac{\chi_c^2\overline{C}_0^2 H_0^2 h^4}{\rho_0\bar{\epsilon}\,\nu^2 h_s^2}. \qquad (5)$$

The first, B the barometric number [21] is due to the solutal buoyancy and is a measure for the relative importance of gravity and viscosity effects, where $\alpha_c = \rho^{-1}(\partial\rho/\partial c)$ is the coefficient of solutal expansion. The magnetic buoyancy has been neglected. The second number B_m, which we call the magnetic barometric number, is due to the presence of the magnetic field (Kelvin force) and describes the relative importance of magnetic and viscosity effects. It depends quadratically on the strength of the magnetic field and is positive irrespective the orientation of the field with respect to gravity. As we will show below this contribution drives the convective instability.

The magnetostatic equation (4) for the ferrofluid contains the dimensionless parameter M_3, which is a measure for the nonlinearity of the magnetization curve. Expanding the magnetic susceptibility around its value at the field H_0, $M_3 = (1+\chi_0)/\bar{\epsilon}$ [9] (with $\bar{\epsilon} = 1 + \chi_0 + \chi_H H_0^2$, $\chi_H = 2\partial\chi/\partial H^2$ and $\chi_0 = \chi(H_0)$). Generally M_3 is rather close to unity and since its influence on the instability is rather weak, we always take a constant value of $M_3 = 1.1$. Outside the sample the magnetic potential obeys the Laplace equation $\Delta\phi_e = 0$.

On the horizontal boundaries at $z = \pm 1/2$, there are the boundary conditions

$$\boldsymbol{v} = 0, \qquad (6)$$

$$\nabla_z(C - M_f\nabla_z\phi) = -1 \qquad (7)$$

$$\bar{\epsilon}\,(\nabla_z\phi - C) = \nabla_z\phi_e \qquad (8)$$

$$\nabla_{x,y}\phi = \nabla_{x,y}\phi_e \qquad (9)$$

describing non-slip velocity, impermeability of the concentration current, longitudinal continuity of the magnetic induction, and transverse continuity of the magnetic field, respectively. Eq. (7) contains the sedimentation current in dimensionless form on the right hand side.

III. GROUND STATE

We can easily find the solution that corresponds to a motionless ferrofluid. In this case the concentration and the magnetic potential only depend on z. Using Eqs. (4) and (7)

$$C(z) = \frac{h_s}{h} + \frac{z}{M_f - 1} \qquad (10)$$

$$\nabla_z\phi = -\frac{h_s\bar{\epsilon}}{h\chi_c\bar{C}_0} + \frac{z}{M_f - 1} \qquad (11)$$

This solution corresponds to the case when the ferrofluid has enough time to accommodate its concentration distribution to both, gravity and magnetic field (via magnetophoresis). However, the time scale of this stratification process ($Sc/M_f \sim 10^5$ for typical ferrofluids) is very long compared to that of the evolution of the instability above the threshold, which is of order unity in the present scaling. Thus, applying a field above the threshold starts the instability development before the state (10) is reached. The state immediately after applying the field, when magnetophoresis is not yet operative,

$$C(z) = \frac{h_s}{h} - z \quad \text{and} \quad \nabla_z\phi = -\frac{h_s\bar{\epsilon}}{h\chi_c\bar{C}_0} - z \qquad (12)$$

is the relevant ground state for experiments. It does not fulfill the boundary condition (7) indicating that there is a small boundary layer, which is not stationary, but evolves (on a long time scale) into the state (10), if the applied field is below the threshold. Using the approximate stationary state (12), instead of the true long time solution as starting point for the instability, is very similar in spirit to what has been done in [8–10], where the huge separation of thermal and solutal time scales has been important.

IV. LINEAR STABILITY

We start from the approximate, but relevant ground state (12) with the effective boundary condition $\nabla_z c_0 = -1$. To study the linear stability of this state we consider perturbations (subscript 1) of the ground state. We expand them into Fourier series in lateral directions $\sim e^{i\boldsymbol{k}\cdot\boldsymbol{r}+\lambda t}$ ($\boldsymbol{r} = (x,y)$) and study the stability of each mode independently. This is possible, since the equations are homogeneous in lateral directions and linearized. Taking the z component of the $curl$ of Eq. (3) and using Eqs. (2,4) the linear evolution equations of the perturbations are

$$\lambda\triangle w = Bk^2 c_1 + B_m k^2(\nabla_z\phi_1 - c_1) + \triangle^2 w \qquad (13)$$

$$\lambda c_1 - w = \frac{1}{Sc}\Delta(c_1 - M_f\nabla_z\phi_1) \qquad (14)$$

$$\nabla_z c_1 = (\nabla_z^2 - M_3 k^2)\phi_1 \qquad (15)$$

with $w = v_z$, the z component of the velocity, and the Laplace operator, $\triangle = (\nabla_z^2 - k^2)$. The external magnetic potential can be expressed in terms of the internal one [9], $\phi_e(\boldsymbol{r}, z) = \exp(k/2)\exp(\mp kz)\phi(\boldsymbol{r}, z = \pm 1/2)$. This allows to write the boundary conditions (6-8) in closed form (without ϕ_e)

$$w = \nabla_z w = 0 \tag{16}$$

$$(1 - M_f)\nabla_z c_0 = -1 \tag{17}$$

$$\nabla_z(c_1 - M_f \nabla_z \phi_1) = 0 \tag{18}$$

$$\bar{\epsilon}\,(\nabla_z \phi_1 - c_1) \pm k\phi_1 = 0 \tag{19}$$

The growth rate λ is the eigenvalue of the homogeneous boundary-value problem, for which this problem has a nontrivial solution. If there is at least one set of values (λ, k) with a positive real part of λ, then the system is linearly unstable. The lowest value of the external field, for which λ reaches zero, denotes the breakdown of linear stability, and the corresponding value of k describes the critical mode. Above the threshold, the k value appropriate to the maximum positive real part of λ defines the most unstable mode.

V. APPROXIMATE SOLUTION OF THE LINEAR STABILITY PROBLEM

The exact solution of the boundary value problem is possible only numerically. Such a numerical solution is not a complicated task, but it is not easy to analyze the material parameter dependence of the results. That is why we prefer an approximate analytical solution, in particular we make use of $Sc \gg 1$, which allows to neglect the r.h.s. of Eq. (14), except for the case, when k^2 is very large. As a consequence of the very slow diffusion small boundary layers occur, which allow to fulfill the boundary condition (18) for $M_f \neq 0$. In the Appendix we show that the only consequence of these boundary layers is the reduction of the boundary condition (18) to an effective one, $\nabla_z c_1 = 0$.

Taking as trial function for the velocity field with the appropriate boundary behavior

$$w = A\cos^2(\pi z), \tag{20}$$

where A is a constant amplitude, the approximated concentration field is $c_1 = (1/\lambda_+)w$ with $\lambda_+ = \lambda + \frac{1}{Sc}k^2$. Substituting this concentration field into the equation for the magnetic field (15), together with the boundary conditions, the perturbation of the magnetic potential is of the form

$$\nabla_z \phi_1 = -\frac{A}{2\lambda_+}\frac{4\pi^2}{4\pi^2 + a^2}\Big(\cos(2\pi z) + \frac{a\bar{\epsilon}\cosh(az)}{a\bar{\epsilon}\cosh(\frac{a}{2}) + k\sinh(\frac{a}{2})}\Big) \tag{21}$$

where $a^2 = M_3 k^2$. Using a Galerkin type procedure Eq. (13) renders the solvability condition that allows a nontrivial solution. Multiplying this equation by $\cos^2(\pi z)$ and integrating over space one finds

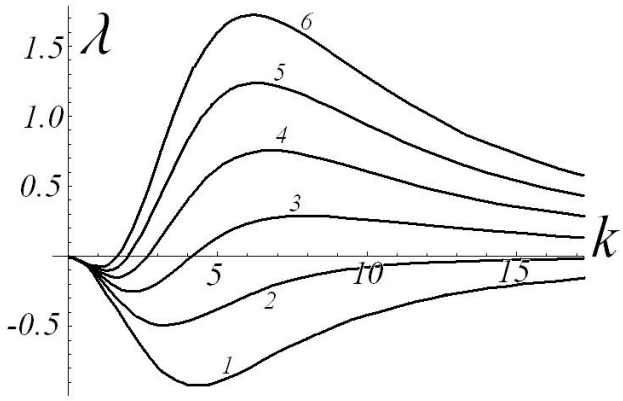

FIG. 1: The linear growth rate λ vs the wave number k for $B_m = 50, 100, 150, 200, 250, 300$ (curves 1-6, respectively) and $B = 100$, $Sc = 10^5$. The curves are numerical solutions of Eq. (22).

$$(3k^2 + 4\pi^2)\lambda\,\lambda_+ + (3k^4 + 8k^2\pi^2 + 16\pi^4)\lambda_+ + 3k^2(B - B_m) + k^2 B_m \frac{4\pi^2 f(k)}{4\pi^2 + a^2} = 0, \tag{22}$$

where the function $f(k)$ is given by

$$f(k) = 1 + \frac{(4\pi)^2}{4\pi^2 + a^2}\,\frac{\bar{\epsilon}a\sinh(\frac{a}{2})}{\bar{\epsilon}a\cosh(\frac{a}{2}) + k\sinh(\frac{a}{2})}$$

This defines implicitly the dependence of the growth rate λ on the wave number k and the parameters B, Sc, M_3, and B_m, and thus on the external field strength.

For $Sc \to \infty$ it is easy to see that the instability starts when $B_m \geq B$ with $k \to \infty$, since the last term in Eq. (22) is constant for large k. For finite Sc the critical threshold and wavevector are

$$B_m^c = B\left(1 + \left[\frac{12\pi^4}{Sc\,M_3^2\,B}\right]^{1/3}\right) \tag{23}$$

$$k_c^6 = \frac{2\pi^2}{3}\frac{Sc\,B}{M_3} \tag{24}$$

with the latter being finite but rather large. Very close to onset the growth rate $\lambda \approx (B_m - B_m^c)/k_c^2$ is small, not only because it is proportional to $B_m - B_m^c$, but also because k_c is large. Therefore, slightly above the threshold the instability grows very slowly and is probably hardly detectable [22]. Well above the threshold (for a finite difference $B_m - B$) it is more involved to find analytically the most unstable mode by maximizing the full expression (22). Therefore a numerical solution of Eq. (22) for the growth rate λ as a function of the wave number k is shown in the Fig. 1. Already for B_m somewhat larger than B the wave number of the most unstable mode is no longer very large, e.g. $k \approx 6$ for $B_m > 200$. In addition, the growth rate is of order 1 in that case. For $B_m < B$ there is no linear instability and λ is negative for all k.

VI. NONLINEAR BEHAVIOR

To investigate amplitudes and patterns of the variables in the unstable regime, one has to use a nonlinear theory. We employ a numerical method of a Galerkin type described in detail in [9]. For the flow pattern we assume one-dimensional convection rolls

$$v_z(x,y,z,t) = w_1(z,t)\cos(kx), \quad (25)$$

$$C(x,y,z,t) = \frac{h}{h_s} + c_0(z,t) + c_1(z,t)\cos(kx), \quad (26)$$

$$\phi(x,y,z,t) = \phi_0(z,t) + \phi_1(z,t)\cos(kx) \quad (27)$$

with the wavelength k taken as the most unstable mode derived in the preceding section. The functions with subscript 0 are not just the ground state solutions (10), since they are modified by the nonlinear feedback. Substituting this form of the fields into Eqs. (2-4) and sorting for the different x dependencies yields the following system of equations

$$(\frac{\partial}{\partial t} - \triangle)\triangle w = Bk^2 c_1 - B_m k^2(\nabla_z\phi_1 - c_1)\nabla_z c_0 \quad (28)$$

$$\frac{\partial}{\partial t}c_1 + w\nabla_z c_0 = \frac{1}{Sc}\Delta(c_1 - M_f\nabla_z\phi_1) \quad (29)$$

$$\frac{\partial}{\partial t}c_0 + \frac{w}{2}\nabla_z c_1 = \frac{1}{Sc}(1 - M_f)\nabla_z^2 c_0 \quad (30)$$

$$\nabla_z c_1 = (\nabla_z^2 - M_3 k^2)\phi_1 \quad (31)$$

where we have neglected $\sin(2kx)$ and $\cos(2kx)$ contributions. The field ϕ_0 has already been eliminated with the help of $\nabla_z^2\phi_0 = \nabla_z c_0$, Eq. (4). To solve Eqs. (28-31) we use vertical profiles of the form

$$w_1(z,t) = A(t)\cos^2(\pi z), \quad (32)$$

$$c_0(z,t) = \frac{-z}{1-M_f} + \sum_{n=1}^{n=N} a_n(t)\sin(2n+1)\pi z, \quad (33)$$

$$c_1(z,t) = \sum_{n=0}^{n=N} b_n(t)\cos 2n\pi z, \quad (34)$$

$$\phi_1(z,t) = d_0(t)\,z + \sum_{n=1}^{n=N}\frac{d_n(t)\sin 2\pi n z}{2\pi n} \quad (35)$$

which satisfy the boundary conditions Eqs. (16-19), identically, if $d_0(\bar{\epsilon} + k/2) - \bar{\epsilon}b_0 + \bar{\epsilon}\sum_{n=1}^{N}(-)^n(d_n - b_n) = 0$ is chosen.

In Fig. 2 the amplitude of the velocity field w_1 is shown as a function of time for different values of B_m. Initially the amplitudes grow exponentially with the linear growth rate λ. In all cases the final flow at long times is stationary. For intermediate times the amplitudes saturate and then decrease considerably. The huge difference between the high peak value and the very small, saturated one can be explained as follows. At the beginning the ferrofluid is stratified showing a concentration gradient, and applying a magnetic field the Kelvin force leads to the instability. While the convective flow grows, it effectively reduces the concentration gradient. The stationary

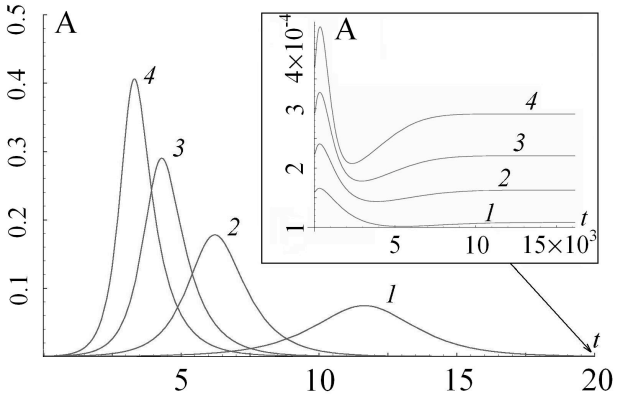

FIG. 2: The amplitude of the velocity w_1 vs time with $B = 100$, $Sc = 10^5$, $M_f = 0.1$, and $B_m = 150, 200, 250, 300$ (curves 1-4, respectively). The inset magnifies the long time behavior. The number of modes has been $N = 30$.

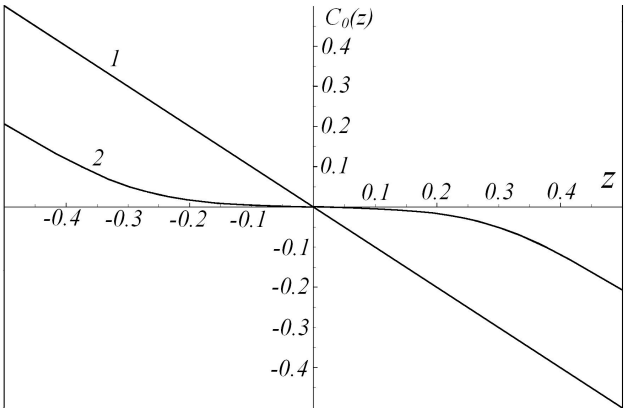

FIG. 3: The profile of the concentration field $c_0(z)$ in the final state (2) as compared to the initial, linear profile (1).

state is reached when the process of building up the concentration gradient is balanced by its destruction due to the flow advection. Since the former process is very slow, only a very small velocity is necessary. This is exactly what is shown in Fig. 2, where the final amplitude of the velocity is very small. The effective reduction of the concentration gradient in the saturated state is demonstrated in Fig. 3. In contrast to the velocities the amplitudes of the concentration variations are not small. From our numerical results we get $c_1 \sim 0.1$ in the stationary state, which is about 10% of the concentration variation due to the stratification process.

We note that the nonlinear part of the Kelvin force (the $c_1\nabla_z c_0$ term in Eq. (28)) plays an important role for the nonlinear behavior of the system, since it changes qualitatively the stationary states reached, as well as the transient behavior. This is because the stationary concentration profile, as shown in Fig. 3, is essentially neither linear nor constant. This is in marked contrast to the thermal convection problem considered in [8–10].

VII. DISCUSSION

In this section we discuss the magnitude of the critical magnetic field necessary to observe the instability. As was shown in Sec. V, the instability takes place if $B_m \gtrsim B$. Using the definitions (5) we get for the threshold value of the (local) magnetic field

$$H_0^2 = \frac{\alpha_c g \rho_0 \bar{\epsilon} h_s}{\chi_c^2 \bar{C}_0} \tag{36}$$

For typical ferrofluids [1, 6] the concentration of the colloidal particles is $\bar{C}_0 \sim 0.07$, the magnetic susceptibility is $\chi \sim 1$ ($\bar{\epsilon} = 1 + \chi \sim 2$), and the mass density is $\rho_0 \sim 10^3\, kg/m^3$. To estimate the coefficient of solutal expansion $\alpha_c = \rho^{-1}(\partial\rho/\partial c)$ we take the concentration dependence of the density as $\rho_0 = (1 - \bar{C}_0)\rho_s + \rho_m \bar{C}_0$, where ρ_s is the density of the solvent and ρ_m is the density of the magnetic particle. We assume $\rho_m \sim 4\rho_s$, which is reasonable for cobalt particles in water, since the density of cobalt is about five times that of water and the surfactant shell of the cobalt particle reduces somewhat the apparent density of the particle. With this assumptions we get $\alpha_c \sim 3$. We also assume the magnetic susceptibility to be directly proportional to the concentration of the magnetic particles, thus neglecting nonlinear effects and the magnetic susceptibility of the solvent. In this case we get $\chi_c \sim 15$.

Finally, we need to find the value of the sedimentation length h_s. Using the expression $h_s = k_B T/(m_p g)$ given in the beginning of section II the buoyant particle mass is estimated as $m_p = \pi d_p^3 \rho_m/6$, with a typical diameter of the magnetic particle $d_p \sim 10\, nm$. With that we get $h_s \sim 20\, cm$.

Substituting these numbers into Eq. (36) we get the threshold value of the magnetic field $H_0 \sim 20\ Gauss$ or in standard units $H_0 \sim 2\, kA/m$. The external field strength to produce such a field locally is about a factor of 2 larger. This means that the instability discussed in this manuscript can be observed experimentally by rather moderate and easily obtainable field strengths. In addition, it shows that our assumption holds that we are in the linear magnetization regime, since non-linear effects in the magnetization curve are observed typically above $H \sim 10\, kA/m$, only.

The time scales involved are also in the practical range. For a kinematic viscosity of $10^{-2}\, cm^2/sec$ for a kerosene based ferrofluid [1], a linear growth rate of $\lambda \sim 1$ translates into characteristic times of $10^{-2}\ sec$ - $10^2\ sec$ for sample thicknesses of $100\,\mu$ - $1\, cm$, respectively. The typical dimensionless time between the steep increase and the subsequent decrease of the nonlinear convection amplitude of ca. 10 (just above threshold, cf. Fig. 2), renders physical times of $10^{-1}\ sec$ - $10^3\ sec$, accordingly.

If one takes magnetorheological fluids (MRF) instead of ferrofluids, we expect the described effects to be much stronger (the sedimentation length and the threshold field to be smaller) because of the strong sedimentation process in MRF. In MRF, however, one has to take into account additionally the magnetic field dependence of the viscosity and the anisotropy of the viscous stress tensor due to the formation of internal structures by the particles.

APPENDIX: BOUNDARY LAYER

In this appendix we show that the concentration current (r.h.s. of Eq. (14)) influences the solution of the linear stability problem in very thin boundary layers, only. To investigate these boundary layers we write the concentration and the magnetic potential as a sum of the bulk solutions ($c_1 = (1/\lambda_+)w$ and ϕ_1 given in Eq. (21)) and boundary layer contributions (c_{bl} and ϕ_{bl}). These are rapidly decaying functions $\sim \exp(q[\pm z - 1/2])$ near the plates at $z = \pm 1/2$, where $1/q$ is a measure for the width of the boundary layers. Applying Eqs. (14,15) to both parts of the variables (and not just to the bulk ones) and assuming the z derivatives of the boundary layer parts to be much larger than those of the bulk ones, one immediately gets the implicit equation for q

$$\lambda\, Sc(q^2 - a^2) = (q^2 - k^2)(q^2[1 - M_f] - a^2). \tag{37}$$

Already somewhat above the threshold the approximate solution $q^2 \approx \lambda\, Sc/(1 - M_f)$ is indeed a very large number.

The amplitudes of the boundary layer functions are related by Eq. (15), $\phi_{bl} \sim q\, c_{bl}$. This allows to reduce the boundary condition (18) to that used in the main text ($\nabla_z c_1 = 0$) and gives $c_{bl} \sim \phi_1/q$. Finally, the boundary condition (19) contains in leading order the bulk functions only, while the boundary layer functions are a small correction of order $1/q$.

[1] R.E. Rosensweig, Ferrohydrodynamics (Cambridge University Press, Cambridge 1985).
[2] B.A. Finlayson, *J. Fluid Mech.* **40**, 753 (1970).
[3] C.L. Russell, P.J. Blennerhassett, and P.J. Stiles, *J. Magn. Magn. Mater.* **149**, 119 (1995).
[4] A. Recktenwald and M. Lücke, *J. Magn. Magn. Mater.* **188**, 326 (1998).
[5] G.K. Auernhammer and H.R. Brand, *Eur. Phys. J. B* **16**, 157 (2000).
[6] S. Odenbach, *Magnetoviscous Effects in Ferrofluids* (Springer, Berlin 2002).
[7] M.I. Shliomis and M. Souhar, *Europhys. Lett.* **49**, 55 (2000).
[8] A. Ryskin, H.-W. Müller, and H. Pleiner, *Phys. Rev. E* **67**, 046302 (2003).
[9] A. Ryskin and H. Pleiner, *Phys. Rev. E* **69**, 046301 (2004).
[10] A. Ryskin and H. Pleiner, *Phys. Rev. E* **71**, 056303 (2005).
[11] J.K. Platten and J.C. Legros, *Convection in Liquids* (Springer, Berlin 1984).
[12] M.C. Cross and P.C. Hohenberg, *Rev. Mod. Phys.* **49**, 581 (1993).
[13] M. Lücke, W. Barten, P. Büchel, C. Fütterer, S. Hollinger, and C. Jung, *Pattern formation in binary fluid convection and in sys-*

tem with throughflow. In "Evolution of Spontaneous Structures in Continuous Systems" (ed. by F.H. Busse and S.C. Müller, Springer, Berlin) *Lecture Notes in Physics* **55**, 127 (1998).

[14] A. Bozhko and G. Putin, *Magnetohydrodynamics* **30**, 147 (2003).

[15] A. Bozhko, G. Putin, E. Beresneva, and P. Bulychev, *Z. Phys. Chem.* **220**, 1 (2006).

[16] T. Tynjälä, A. Bozhko, P. Bulychev, G. Putin, and P. Sarkomaa, *J. Magn. Magn. Mater.* **300**, 195 (2006).

[17] T. Biben, J.-P. Hansen, and J.-L. Barrat, *J. Chem. Phys.* **98**, 7330 (1993).

[18] E. Blums, *J. Magn. Magn. Mater.* **252**, 189 (2002).

[19] There are two typos in Eq. (25) of [9]: α_c and α_H should come with a minus sign in front; the subsequent Eq. (42), however, is correct.

[20] At $M_f = 1$ our description would break down as discussed in [9] for M_2.

[21] M.I. Shliomis and B.L. Smorodin, *Phys. Rev. E* **71**, 036312 (2005).

[22] In that case the role of field-induced stratification due to magnetostriction (M_f) cannot be neglected, neither in the ground state nor in the dynamics of its perturbations.